

Intersubband electronic Raman scattering in narrow GaAs single quantum wells dominated by single-particle excitations *

Takeya Unuma,^{1,†} Kensuke Kobayashi,¹ Aishi Yamamoto,² Masahiro Yoshita,¹ Yoshiaki Hashimoto,¹ Shingo Katsumoto,¹ Yasuhiro Iye,¹ Yoshihiko Kanemitsu,^{2,‡} and Hidefumi Akiyama¹

¹ *Institute for Solid State Physics, University of Tokyo,
and CREST, JST, Kashiwa, Chiba 277-8581, Japan*

² *Graduate School of Materials Science, Nara Institute of Science and Technology, Ikoma, Nara 630-0192, Japan*

(Dated: 8 June 2004)

We measured resonant Raman scattering by intersubband electronic excitations in GaAs/AlAs single quantum wells (QWs) with well widths ranging from 8.5 to 18 nm. In narrow (less than ~ 10 nm) QWs with sufficiently high electron concentrations, only single-particle excitations (SPEs) were observed in intersubband Raman scattering, which was confirmed by the well-width dependence of Raman spectra. We found characteristic variations in Raman shift and line shape for SPEs with incident photon energy in the narrow QWs.

Intersubband electronic excitations in quantum wells (QWs) are strongly affected by many-body Coulomb interactions¹. In electronic Raman scattering in doped QWs, two types of intersubband collective excitations have been confirmed by many researchers² since the first reports by Abstreiter and Ploog³ and by Pinczuk *et al.*⁴ in 1979: a collective charge-density wave (CDW) appears if the polarizations of incident and scattered lights are parallel (\parallel), whereas a collective spin-density wave (SDW) appears if they are crossed (\perp).

The CDW and SDW excitation energies are given by^{1,5}

$$E_{\text{CD}} \approx E_{10} + (\alpha - \beta)N_S, \quad (1)$$

$$E_{\text{SD}} \approx E_{10} - \beta N_S \quad (2)$$

based on the local-density functional theory^{6,7,8}, where N_S is the sheet electron concentration in a QW, E_{10} is the intersubband energy separation that includes static many-body corrections, and αN_S and βN_S are dynamical many-body corrections (called the depolarization shift and excitonic shift) due to the direct and exchange-correlation intersubband Coulomb interactions, respectively. In the crudest approximation^{8,9}, the depolarization shift αN_S is proportional to $N_S d_{\text{eff}}$ and the excitonic shift βN_S is proportional to $(N_S/d_{\text{eff}})^{1/3}$, where d_{eff} is the effective well width¹. Experimentally, αN_S can be determined from the measured value of $E_{\text{CD}} - E_{\text{SD}}$; βN_S can be estimated only when there is information about E_{10} .

Later, in 1989, Pinczuk *et al.* reported¹⁰ that not only CDW and SDW but also single-particle excitations (SPEs) are observed in intersubband electronic Raman scattering and their transition energy is E_{10} for modulation-doped 25-nm GaAs/Al_{0.3}Ga_{0.7}As single QWs with $N_S = (1.5-3) \times 10^{11} \text{ cm}^{-2}$. SPEs are observed for both the parallel and crossed polarizations and seem to become stronger^{10,11} at higher values of N_S .

There are many other reports on intersubband electronic Raman scattering for wide (more than ~ 20 nm) GaAs QWs. It will be interesting to measure Raman scattering also in narrower QWs, considering $\beta/\alpha \sim (N_S d_{\text{eff}})^{-2/3}$. However, there are only a few reports for narrower GaAs QWs^{12,13} because interface roughness makes Raman peaks broader and more difficult to observe. To our knowledge, such an experiment has never been reported for a single QW.

In this paper, we report resonant Raman scattering by the lowest ($0 \rightarrow 1$) intersubband electronic excitations in a set of modulation-doped GaAs/AlAs single QWs with well widths ranging from 8.5 to 18 nm. We found unexpected results that parallel- and crossed-polarization Raman spectra of narrow QWs had only a single peak at almost the same energy, though electron concentrations in the QWs were high enough that the theoretical values of the depolarization shift were more than 10 meV. On the other hand, spectra of a wide QW had a typical feature in that CDW, SDW, and SPE peaks all appeared clearly. In an intermediate-width QW we found no SDW peak, a very small CDW peak, and large SPE peaks, which led us to conclude that the peaks observed in narrow QWs correspond to the SPEs. Moreover, characteristic variations in Raman shift and line shape with incident photon energy were observed commonly in the narrow QWs. They were found to have a correlation with resonance strength and can be qualitatively understood by considering relaxation of the in-plane wave-vector conservation rule.

The samples used in this study were *n*-type modulation-doped GaAs/AlAs single QWs grown by molecular beam epitaxy on (001) GaAs substrates: N1, N2, W, and M. Their well widths L ranged from 8.5 to 18 nm, as shown in Table I. The QW structure of sample N1, for example, consisted of a Si-doped Al_{0.33}Ga_{0.67}As layer, a 4.0-nm undoped Al_{0.33}Ga_{0.67}As spacer layer, a 6.0-nm undoped AlAs barrier, a 10-nm undoped GaAs QW, a 6.0-nm undoped AlAs barrier, and a Si-doped Al_{0.33}Ga_{0.67}As layer. The other samples had similar QW structures. The samples were designed such that cal-

*submitted to Phys. Rev. B.

TABLE I: Main parameters of the samples. L is the well width, N_S is the sheet electron concentration, and μ is the mobility at 4.2 K. Theoretical values of the depolarization shift are calculated after Ref. 1.

Sample	Well/barrier	L (nm)	N_S (10^{12} cm^{-2})	μ ($10^4 \text{ cm}^2/\text{Vs}$)	Calculated depolarization shift (meV)
N1	GaAs/AlAs	10	1.2	4.3	11
N2	$\text{In}_{0.1}\text{Ga}_{0.9}\text{As}/\text{AlAs}$	8.5	2.0	2.8	14
W	GaAs/AlAs	18	0.63	44	9
M	GaAs/AlAs	13.5	1.1	5.6	12

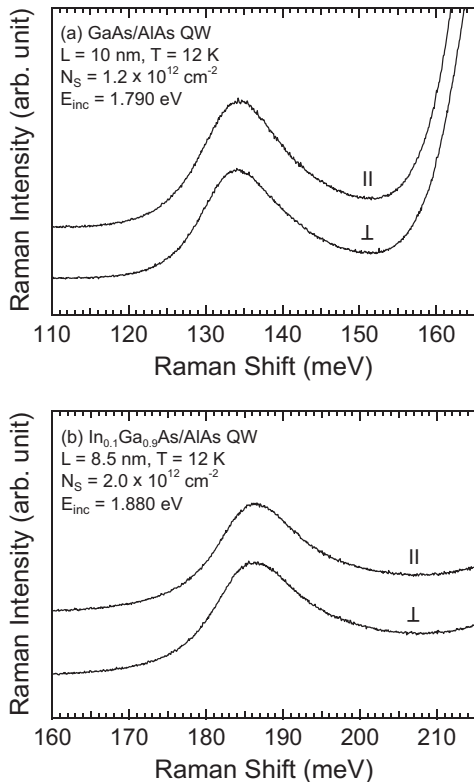


FIG. 1: Intersubband electronic Raman spectra of (a) 10-nm GaAs/AlAs (sample N1) and (b) 8.5-nm $\text{In}_{0.1}\text{Ga}_{0.9}\text{As}/\text{AlAs}$ (sample N2) single QWs at 12 K. The \parallel and \perp marks mean that incident- and scattered-light polarizations were parallel and crossed, respectively.

culated values of the depolarization shifts¹ were more than 10 meV, which is larger than the linewidths of intersubband transition¹⁴ and large enough to see in Raman spectra. The electron concentrations were controlled mainly by the thickness of spacer layers. Exceptionally, $\text{In}_{0.1}\text{Ga}_{0.9}\text{As}$ alloy was used for the QW layer of sample N2 in order to raise its electron concentration sufficiently. The sheet electron concentrations N_S and mobilities μ at 4.2 K are also shown in Table I. The values of N_S were confirmed by Shubnikov-de Haas measurements for samples N1, W, and M, and by Hall measurements for sample N2.

Raman spectra were measured at 12 K in a geometry of back-scattering normal to QW layers such that in-plane

wave-vector transfer from an incident photon to an electron was less than $\sim 10^4 \text{ cm}^{-1}$. Typical values of incident laser power and spot size were 30 mW and 0.3 mm^2 , respectively. Finding a suitable resonance condition is crucial for electronic Raman experiments in order to make Raman signals intensified and avoid their overlap with the strong photoluminescence (PL) from the GaAs QW or AlGaAs layers. In our experiments, the incident photon energies E_{inc} were probably resonant with the energy gap between the electron first-excited (E_1) subband and the heavy-hole second-excited (H_2) subband in a GaAs QW¹⁵. This was the only resonance condition that made intersubband Raman scattering observable in the energy range between the PL peak positions for the QW and AlGaAs layers in samples N1, N2, and M.

Figure 1 (a) shows typical intersubband Raman spectra of sample N1. The backgrounds of the spectra were due to PL from the QW. The parallel- and crossed-polarization spectra have only a single peak at almost the same energies of 134.2 meV and 134.0 meV, respectively, while the theoretical value of the depolarization shift calculated after Ref. 1 was about 11 meV for the QW with $N_S = 1.2 \times 10^{12} \text{ cm}^{-2}$. A similar polarization dependence was observed in sample N2, as shown in Fig. 1. (b), where $N_S = 2.0 \times 10^{12} \text{ cm}^{-2}$ and the calculated depolarization shift was 14 meV. Apparently, these experimental results do not correspond to the conventional interpretation for wide QWs that CDW and SDW peaks are in the parallel- and crossed-polarization spectra, respectively, and their energy difference is the depolarization shift. We assigned the Raman peaks in Fig. 1 to SPEs, which was confirmed by the well-width dependence of Raman spectra as discussed in later paragraphs.

The resonance condition for sample N1 had an allowable range of about 70 meV in the vicinity of $E_{\text{inc}} = 1.80 \text{ eV}$ due to the electron Fermi distribution and the relaxation of the in-plane wave-vector conservation rule caused by interface roughness or other scatterers. In this range, we measured Raman spectra of sample N1 and found peculiar variations in Raman shift and line shape with incident photon energy. Similar characteristics were also found in sample N2.

Figure 2 shows the spectra of sample N1 at various incident photon energies E_{inc} : (a) 1.790 eV, (b) 1.807 eV, (c) 1.817 eV, and (d) 1.835 eV. In Fig. 2 (a), the parallel- and crossed-polarization spectra have almost the same peak positions. In Fig. 2 (b), however, the crossed-polarization spectrum has a slightly

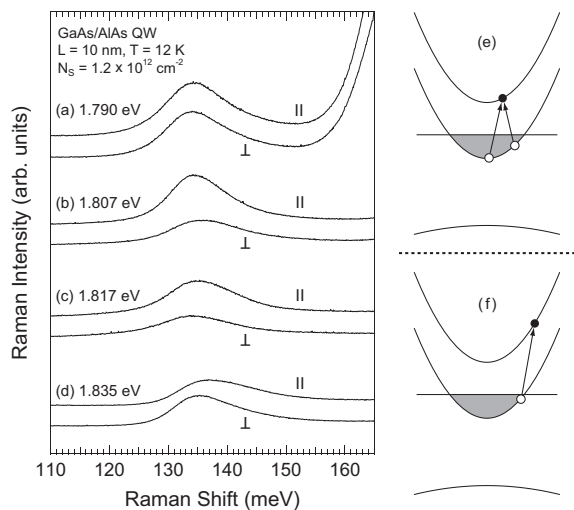


FIG. 2: Intersubband electronic Raman spectra of a 10-nm GaAs/AlAs QW (sample N1) at various incident photon energies E_{inc} : (a) 1.790 eV, (b) 1.807 eV, (c) 1.817 eV, and (d) 1.835 eV. \parallel : parallel polarizations, \perp : crossed polarizations. (e) and (f) are schematic diagrams of intersubband electronic excitations with the relaxation of the in-plane wave vector conservation rule at low and high E_{inc} , respectively.

higher peak position than the parallel-polarization spectrum. In Fig. 2 (c), on the other hand, the parallel-polarization spectrum has a slightly higher peak position than the crossed-polarization spectrum. In Fig. 2 (d), the parallel-polarization spectrum again has a slightly higher peak position than the crossed-polarization spectrum, and their line shapes are very asymmetric. Note, on the whole in Fig. 2, that the polarization dependence of the peak position at each E_{inc} is small compared with the theoretically expected depolarization shift of 11 meV, and that the Raman shift of the peak position for the parallel polarizations becomes larger as E_{inc} increases from 1.790 to 1.835 eV.

Figure 3 shows the Raman shifts of peak position (circles) and the Raman integrated intensities (squares) versus incident photon energies in sample N1. Open and closed symbols correspond to the values for the parallel and crossed polarizations, respectively. In Fig. 3, there is a correlation between the Raman shift and the integrated intensity: the Raman shift becomes smaller as the resonance gets stronger. Near $E_{\text{inc}} = 1.81$ eV, where the Raman shift is larger for the crossed polarizations than for the parallel polarizations, the resonance curve for the crossed polarizations has a dip. At $E_{\text{inc}} = 1.83 - 1.85$ eV, where spectra have larger Raman shifts and very asymmetric line shapes as shown in Fig. 2 (d), the resonance is weaker for both the parallel and crossed polarizations.

Next, to clarify the origin of the intersubband Raman peaks observed in samples N1 and N2, we also measured Raman spectra in wider QWs with well widths of 18 nm (sample W) and 13.5 nm (sample M) and investigated

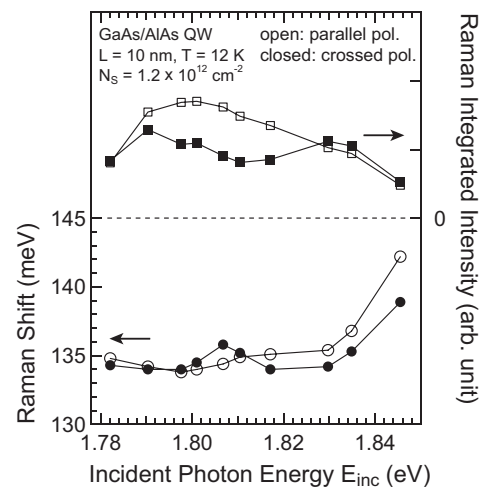


FIG. 3: Raman shift of peak position and Raman integrated intensity versus incident photon energy in a 10-nm GaAs/AlAs QW (sample N1). Open and closed symbols show the values for the parallel- and crossed-polarization spectra, respectively.

how spectral features changed with well width. Figure 4 (a) shows Raman spectra of sample W. The CDW peak at 56.1 meV and the SDW peak at 45.1 meV are clearly seen in parallel- and crossed-polarization spectra, respectively, as well as the SPE peaks at 48.3 meV in both the spectra. The energy difference of 11.0 meV between the CDW and SDW is in good agreement with the theoretical calculation of the depolarization shift. This is a conventional result that follows Refs. 10, 11, and other reports.

Figure 4 (b) shows Raman spectra of sample M, which had an intermediate well width: the large SPE peaks at 69.5 meV for both polarizations and the small CDW peak at 81.8 meV for the parallel polarizations. (Sharp peaks at 72.6 meV and 69.8 meV for the parallel polarizations are from 2-LO-phonon excitations in GaAs and AlGaAs layers, respectively.) The SDW peak is not seen, probably because it is too small or overlapped by the SPE peak. The change in spectral features with well width shows that the peaks observed in samples N1 and N2 should be assigned to the SPEs.

The electronic Raman process for intersubband SPEs is microscopically described as follows: An electron is excited from a valence band state to a conduction first-excited subband state $(\mathbf{k}_1, E_{10} + \varepsilon(\mathbf{k}_1))$ by an incident photon with the resonant energy E_{inc} , where $\varepsilon(\mathbf{k}) = \hbar^2 \mathbf{k}^2 / 2m^*$ with \mathbf{k} being the electron in-plane wave vector and m^* being the effective mass. Then, an electron in a conduction ground subband state $(\mathbf{k}_0, \varepsilon(\mathbf{k}_0))$ recombines with the virtual hole remaining in the valence band state, which produces a scattered photon with energy E_{scatt} . As the result, an intersubband SPE $(\mathbf{k}_0, \varepsilon(\mathbf{k}_0)) \rightarrow (\mathbf{k}_1, E_{10} + \varepsilon(\mathbf{k}_1))$ occurs.

In a geometry of back-scattering normal to QW layers, basically, the change in the in-plane wave vector

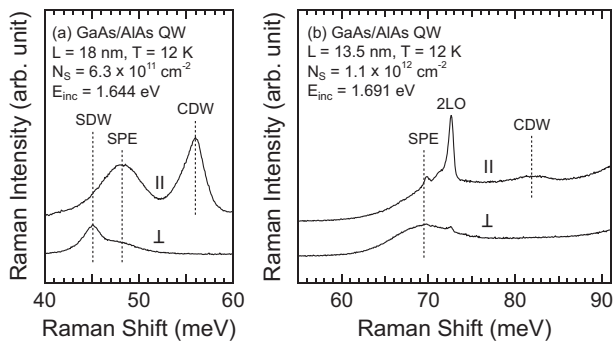


FIG. 4: Intersubband electronic Raman spectra of (a) 18-nm (sample W) and (b) 13.5-nm (sample M) GaAs/AlAs single QWs at 12 K. \parallel : parallel polarizations, \perp : crossed polarizations.

$\mathbf{q} = \mathbf{k}_1 - \mathbf{k}_0$ is 0 and the Raman shift $E_{\text{inc}} - E_{\text{scatt}}$ for the intersubband SPE is E_{10} , since photon in-plane wave vectors are negligible. In fact, there are some dephasing mechanisms that cause broadening of the in-plane wave vectors of the electron and hole states involved, or the relaxation of in-plane wave-vector conservation rule; so $\mathbf{q} \neq 0$ intersubband SPE processes are also allowed.

Figure 2 (e) schematically shows a standard case of $|\mathbf{k}_1| < k_F$ for intersubband SPEs, where k_F is the Fermi wave vector. In this case, various $\mathbf{q} \neq 0$ excitation processes only cause a symmetric width of Raman spectra around E_{10} , which we think corresponds to the case of $E_{\text{inc}} < 1.83$ eV in our experiments. Near the higher limit of E_{inc} for intersubband Raman scattering, however, $|\mathbf{k}_1|$ is more than $\sim k_F$ as shown in Fig. 2 (f). In this case, particular $\mathbf{q} \neq 0$ excitation processes such that $\mathbf{k}_0 \cdot \mathbf{q} > 0$ are dominant and $E_{\text{inc}} - E_{\text{scatt}} > E_{10}$. Thus, Raman spectra have a larger Raman shift and more asymmetric line shape (with a high-energy tail) at $E_{\text{inc}} = 1.83 - 1.85$

eV than at $E_{\text{inc}} < 1.83$ eV. It is not clear at present which carrier state was most deeply involved in the in-plane wave-vector conservation relaxation: the electron ground state, the electron first-excited state, or the virtual hole state.

Recently, Das Sarma and Wang have developed a theory of electronic Raman scattering explicitly considering the intermediate valence band state and the resonant excitation effect based on the random phase approximation (RPA)¹⁶, whereas standard RPA theories use a nonresonant approximation and neglect the intermediate valence band state. They have shown by numerical calculations that SPEs become strong only when the resonant excitation effect is included¹⁶. In our experiments the correlation between Raman shift and Raman integrated intensity with incident photon energy (Fig. 3) suggests that the resonant excitation effect is essential to the observed SPEs, and our results may be explained better by such an advanced theory.

In summary, we have measured intersubband electronic Raman scattering in GaAs/AlAs single QWs with well widths ranging from 8.5 to 18 nm. The change in Raman spectral features with well width shows that only SPEs have been observed in narrow (8.5-nm and 10-nm) QWs for both parallel and crossed polarizations. Variations in Raman shift and line shape with incident photon energy have been found in the narrow QWs and qualitatively explained by considering $\mathbf{q} \neq 0$ intersubband SPEs inside and across k_F .

We are grateful to Professor T. Ando for his helpful discussions about the theory of intersubband electronic Raman scattering. This work was partly supported by a Grant-in-Aid from the Ministry of Education, Culture, Sports, Science and Technology, Japan. One of us (T.U.) also thanks the Japan Society for the Promotion of Science for partial financial support.

[†] unuma@issp.u-tokyo.ac.jp

[‡] Also at: Institute for Chemical Research, Kyoto University, Uji, Kyoto 611-0011, Japan.

¹ T. Ando, A. B. Fowler, and F. Stern, *Rev. Mod. Phys.* **54**, 437 (1982).

² For a review, see A. Pinczuk and G. Abstreiter, *Light Scattering in Solids V*, pp.153 – 211 (Springer-Verlag, 1988).

³ G. Abstreiter and K. Ploog, *Phys. Rev. Lett.* **42**, 1308 (1979).

⁴ A. Pinczuk, H. L. Störmer, R. Dingle, J. M. Worlock, W. Wiegmann, and A. C. Gossard, *Solid State Commun.* **32**, 1001 (1979).

⁵ We define α and β following the convention of Ref. 10. They are related to Ando's convention by $\alpha = \alpha_{\text{Ando}} E_{10} / (2N_S)$ and $\beta = \beta_{\text{Ando}} E_{10} / (2N_S)$.

⁶ W. Kohn and L. J. Sham, *Phys. Rev.* **140**, A1133 (1965).

⁷ L. Hedin and B. I. Lundqvist, *J. Phys. C* **4**, 2064 (1971).

⁸ W. L. Bloss, *J. Appl. Phys.* **66**, 3639 (1989).

⁹ When $r_s = [4\pi a_B^3 n(z)/3]^{-1/3}$ is much less than unity,

where $n(z)$ is the three-dimensional electron concentration and a_B is the Bohr radius in GaAs, the exchange-correlation potential $V_{xc}[n(z)]$ has an approximate dependence of $-1/r_s$, leading to $\beta N_S \sim (N_S/d_{\text{eff}})^{1/3}$.

¹⁰ A. Pinczuk, S. Schmitt-Rink, G. Danan, J. P. Valladares, L. N. Pfeiffer, and K. W. West, *Phys. Rev. Lett.* **63**, 1633 (1989).

¹¹ H. Peric, B. Jusserand, D. Richards, and B. Etienne, *Phys. Rev. B* **47**, 12722 (1993).

¹² G. Abstreiter, T. Egeler, S. Beeck, A. Seilmeier, H. J. Hübner, G. Weimann, and W. Schlapp, *Surf. Sci.* **196**, 613 (1988).

¹³ M. Ramsteiner, J. D. Ralston, P. Koidl, B. Dischler, H. Biebl, J. Wagner, and H. Ennen, *J. Appl. Phys.* **67**, 3900 (1990).

¹⁴ T. Unuma, M. Yoshita, T. Noda, H. Sakaki, and H. Akiyama, *J. Appl. Phys.* **93**, 1586 (2003); T. Unuma, T. Takahashi, T. Noda, M. Yoshita, H. Sakaki, M. Baba, and H. Akiyama, *Appl. Phys. Lett.* **78**, 3448 (2001).

- ¹⁵ G. Danan, A. Pinczuk, J. P. Valladares, L. N. Pfeiffer, K. W. West, and C. W. Tu, Phys. Rev. B **39**, 5512 (1989).
- ¹⁶ S. Das Sarma and D. W. Wang, Phys. Rev. Lett. **83**, 816 (1999); D. W. Wang and S. Das Sarma, Phys. Rev. B **65**, 125322 (2002).